The effects of asymmetric potential vorticity forcing on the instability of South Asia High and Indian summer monsoon onset

ZHANG YaNi[1], WU GuoXiong[2*], LIU YiMin[2] & GUAN Yue[1]

[1] *National Meteorological Center, Beijing 100081, China;*
[2] *State Key Laboratory of Numerical Modeling for Atmospheric Sciences and Geophysical Fluid Dynamics, Institute of Atmospheric Physics, Chinese Academy of Sciences, Beijing 100029, China*

Based on the theory of potential vorticity (PV), the unstable development of the South Asia High (SAH) due to diabatic heating and its impacts on the Indian Summer Monsoon (ISM) onset are studied via a case diagnosis of 1998. The Indian Summer Monsoon onset in 1998 is related to the rapidly strengthening and northward moving of a tropical cyclone originally located in the south of Arabian Sea. It is demonstrated that the rapid enhancement of the cyclone is a consequence of a baroclinic development characterized by the phase-lock of high PV systems in the upper and lower troposphere. Both the intensification of the SAH and the development of the zonal asymmetric PV forcing are forced by the rapidly increasing latent heat released from the heavy rainfall in East Asia and South East Asia after the onsets of the Bay of Bengal (BOB) monsoon and the South China Sea (SCS) monsoon. High PV moves southwards along the intensified northerlies on the eastern side of the SAH and travels westwards on its south side, which can reach its northwest. Such a series of high PV eddies are transported to the west of the SAH continuously, which is the main source of PV anomalies in the upper troposphere over the Arabian Sea from late spring to early summer. A cyclonic curvature on the southwest of the SAH associated with increasing divergence, which forms a strong upper tropospheric pumping, is generated by the anomalous positive PV over the Arabian Sea on 355 K. The cyclone in the lower troposphere moves northwards from low latitudes of the Arabian Sea, and the upper-layer high PV extends downwards and southwards. Baroclinic development thus occurs and the tropical low-pressure system develops into an explosive vortex of the ISM, which leads to the onset of the ISM. In addition, evolution of subtropical anticyclone over the Arabian Peninsula is another important factor contributing to the onset of the ISM. Before the onset, the surface sensible heating on the Arabian Peninsula is very strong. Consequently the subtropical anticyclone which dominated the Arabian Sea in spring retreats westwards to the Arabian Peninsula and intensifies rapidly. The zonal asymmetric PV forcing develops gradually with high PV eddies moving southwards along northerlies on the eastern side of the anticyclone, and a high PV trough is formed in the middle troposphere over the Arabian Sea, which is favorable to the explosive barotropic development of the tropical cyclone into the vortex. Results from this study demonstrate that the ISM onset, which is different from the BOB and the SCS monsoon onset, is a special dynamical as well as thermodynamic process occurring under the condition of fully coupling of the upper, middle, and lower tropospheric circulations.

potential vorticity, South Asian High, diabatic heating, zonal asymmetric instability, summer monsoon onset

---

*Corresponding author (email: gxwu@lasg.iap.ac.cn)

In general, the Asia Summer Monsoon (ASM) onset lasts for about one month: after the onset of the BOB and the SCS successively in early and middle May, the ISM onset occurs in early June over the Indian Peninsula (Wu et al., 1998b; Zhang et al., 1998). Afterwards, the SCS monsoon strengthens and the East Asian monsoon moves northwards to East China, Japan and Korea, and the whole Asia enters summer season. Studies show that the ISM has important impacts on weather and climate in China and is closely related to the commencement of Meiyu over the Yangtze River Valley as well as the precipitation in North China (Liang, 1988; Guo, 1992; Liu et al., 2008a, 2008b; Ding et al., 2008). Therefore, it is important to study the onset of the ISM. The Asian summer monsoon onset is affected not only by the sea surface temperature, the land-/sea-atmosphere interactions in the lower layers, but also by the atmosphere circulation in the middle and upper layers (Wu et al., 2011, 2012; Jiang et al., 2011; Li et al., 2011). In this study, we try to investigate how the SAH evolves after the BOB and SCS summer monsoon onset, and how such an SAH variation affects the ISM onset.

The South Asian monsoon circulation is a zonally asymmetric meridional circulation induced by localized diabatic heating in the tropics and subtropics. Most studies on the zonally averaged meridional circulation are based on the assumption of nonlinear, axisymmetric, and steady flow (Schneider, 1977; Held et al., 1980; Lindzen et al., 1988; Plumb et al., 1992). In a steady, inviscid, and axisymmetric atmosphere, localized heating can drive a meridional circulation provided that absolute angular momentum is conserved, i.e., absolute vorticity vanishes. In other words, an induced upper tropospheric divergent flow cannot cross contours of zero absolute vorticity. At the equator (Held et at., 1980) or near the equator (Lindzen et al., 1988), the above condition is easily met with weak induced relative vorticity because the planetary vorticity vanishes or is very small. Therefore, a weak thermal forcing there will easily drive a meridional circulation. In contrast, when the forcing is localized in the subtropics (Plumb et al., 1992), the planetary vorticity becomes larger. Only if the thermally induced anticyclonic relative vorticity is strong enough to cancel the planetary vorticity can a meridional circulation exist. Thus, there exist an abrupt transition in the thermally induced meridional circulation and a threshold in thermal forcing magnitude. Only when a diabatic heating is stronger than the threshold, can the heating induce relative vorticity to compensate the planetary vorticity, and the meridional circulation be excited. Emanuel (1995) and Zheng (1998) discussed the 'criticality' condition for the occurrence of meridional circulation in response to a subtropical thermal forcing in a moist atmosphere. As far as the asymmetric problem is concerned, Schneider (1987) proved that in an inviscid steady state (with no transient eddies) there can be no net divergence across any contour of nonzero absolute vorticity. Sobel and Plumb (1999) showed that this result holds true for inviscid flow even in the presence of transients, provided the area enclosed by the absolute vorticity contour does not change with time.

Monsoon onset and maintenance are closely related to the formation and evolution of the upper tropospheric anticyclone and the associated divergent flow. According to the aforementioned dynamic constraint, in the upper troposphere the anticyclone must be either unsteady or affected by viscosity since the absolute vorticity and divergent flow is not zero over any finite region. Since in the upper troposphere friction and molecular viscosity are utterly negligible, anything that might loosely be regarded as viscosity must occur through eddy effects and thus, in reality, the upper tropospheric anticyclone must be under unstable state. Recently the studies on the three dimension monsoonal circulation based on the steady, non-linear and axisymmetric theory highlighted that, as the assumption of zonal symmetry is relaxed, transients naturally emerge as an intrinsic feature of the monsoons, and that these disturbances play important roles in the dynamical balance of the associated meridional circulations (Xie et al., 1999; Hsu et al., 2000). Using a shallow-water equation model, Hsu and Plumb (2000) discussed the non-linear dynamics of the upper tropospheric anticyclone under non-axisymmetric conditions, and showed that the anticyclone becomes unstable and periodically sheds eddies into the background flow when the imposed asymmetry is sufficiently large. Analysis based on the NCEP/NCAR reanalysis proves that in summer the evolution of the SAH over the Asian monsoon area does show such an eddy-shedding phenomenon (Popovic et al., 2001). Liu et al. (2007) studied the impacts of thermal forcing of the Tibetan Plateau (TP) on the summer flow over Asia using a global primitive equation model and found that if the heating over the TP is sufficiently strong, low PV eddies detach from the main anticyclone, producing a quasi-biweekly oscillation. This study showed that unstable development of the upper tropospheric anticyclone occurs due to strong diabatic heating.

The outbreak of the Asian summer monsoon first occurs over the eastern coast of the BOB (Wu et al., 1998b; Zhang et al., 1998; Mao, 2001). Liu et al. (Liu et al., 2003a, 2003b) studied the important impacts of condensation heating associated with the BOB monsoon onset on the retreat of the subtropical anticyclone from the SCS and on the SCS monsoon onset. Can the strong latent heating released from the heavy rainfall over the BOB and the SCS after the SCS summer monsoon onset also have strong impacts on the ISM onset? What is the physical mechanism involved? In this paper a case study on the ISM onset in 1998 is conducted and the possible impacts of zonal asymmetric PV forcing due to diabatic heating on both the unstable evolution of the SAH and the ISM onset are investigated. The 1998 case is selected because in this year several atmospheric field experiments in the Asian monsoon regions were carried out and the process of the ASM onset has been well

explored and reported.

1   Data and potential vorticity (PV) theory

The dataset used is the NCEP/NCAR (National Center for Environmental Prediction) reanalysis daily data (Kistler et al., 2001), including surface sensible heat flux, temperature, geopotential height and wind with a spatial resolution of 2.5°×2.5° and 17 vertical levels. Precipitation data are daily rainfall of GPCP（The Global Precipitation Climatology Project）with a spatial resolution of 1°×1°.

PV is a quantity which can jointly depicts the dynamic state and thermodynamic state of the atmospheric particles. Ertel's PV is defined as follows (Ertel, 1942):

$$P_E = \alpha \vec{\zeta}_a \cdot \nabla \theta, \tag{1}$$

where α is specific volume, and $\vec{\zeta}_a$ and θ denote three-dimensional absolute vorticity and potential temperature respectively. If the hydrostatic approximation is made, it is given by

$$P = -g(f + \zeta_\theta)/(\partial P/\partial \theta), \tag{2}$$

and PV equation becomes (Holton, 2004) :

$$\frac{\partial P}{\partial t} + \vec{V} \cdot \nabla_\theta P = \frac{P}{\sigma} \frac{\partial}{\partial \theta}(\sigma \dot{\theta}) + \sigma^{-1} \vec{k} \cdot \nabla_\theta \times \left(\vec{F}_r - \dot{\theta} \frac{\partial \vec{V}}{\partial \theta} \right), \tag{3}$$

where $\sigma = -g^{-1} \partial P/\partial \theta$ is the density in isentropic coordinates, $\dot{\theta}$ is diabatic heating, and $\vec{F}_r$ is friction. Eq. (3) expresses the PV conservation following the motion on isentropic surfaces under frictionless as well as adiabatic constraints. In the tropics and subtropics, the tilting of isentropic surface is small, and the internal forcing associated with slantwise vorticity development can be ignored, then the alternative form of vertical vorticity tendency equation can be obtained from eq. (3) as follows (Wu et al., 1998a; Wu et al., 1999; Liu et al., 1999b; Liu et al., 2001):

$$\frac{\partial \zeta}{\partial t} + \vec{V} \cdot \nabla \zeta + \beta v = (1 - \kappa)(f + \zeta)\frac{\omega}{P} -$$
$$(f + \zeta)\frac{1}{\theta}\frac{d\theta}{dt} + \frac{f + \zeta}{\theta_z}\frac{\partial Q}{\partial z} + S, \tag{4}$$

where S denotes horizontal non-uniform heating and is given by

$$S = -\frac{1}{\theta_z}\frac{\partial v}{\partial z}\frac{\partial Q}{\partial x} + \frac{1}{\theta_z}\frac{\partial u}{\partial z}\frac{\partial Q}{\partial y} = -\frac{g}{f\theta\theta_z}(\nabla_h\theta \cdot \nabla_h Q), \tag{5}$$

and others are common in meteorology. Scale analysis (Wu et al., 1999) shows that in subtropical convective heating areas eq. (4) can be approximately written as:

$$\frac{\partial \zeta}{\partial t} + \beta v \approx \frac{f + \zeta}{\theta_z}\frac{\partial Q}{\partial z}. \tag{6}$$

Therefore, in the upper layers above the maximum heating, geopotential height increases due to negative vorticity generation, or northerly gets strengthened when quasi-steady state is assumed. In other words, subtropical monsoon rainfall can contribute to the SAH strengthening and its westward development. Based on this, we investigate the development and evolution of the SAH after the onset of the SCS monsoon and its impacts on the ISM onset.

2   The circulation characteristics during the ISM onset period in 1998

2.1   Development of the subtropical anticyclone over the Arabian Peninsula and strengthening of a northward traveling tropic cyclone

The onset of the Indian summer monsoon is related generally to the development and northward moving of an explosive vortex over the Arabian Sea (Krishnamurti et al., 1981; Soman et al., 1993). Studies have shown that in 1998 the onset of the ISM occurred on June 7 (Mao, 2001). Figure 1 gives the evolution of daily precipitation, 700 hPa geopotential height and wind, and the ridge line of the 500 hPa subtropical high before and after the IMS onset. On June 4–5 (Figure 1(a) and (b)), in the area north of 15°N the anticyclonic circulation dominates the regions from the Arabian Peninsula and Arabian Sea to Indian Peninsula, and the ridge line of the subtropical anticyclone is zonal orientated continuously. A cyclone near 70°E over the Arabian Sea is located south of 10°N before June 4 (Figure omitted) and moves slightly northwards to north of 10°N on June 4 and 5.

On June 6 this cyclone develops into a vortex and rainfall increases (Figure 1(c)). On June 7, the vortex center moves to north of 15°N, and the 500 hPa ridge line breaks over the east of Arabian Sea. At this time, southerlies extend northwards to the west of Indian Peninsula (Figure 1(d)). After June 7, the vortex moves further northwards and strengthens continuously until it lands. The establishment of southerly, the formation of monsoon trough and the break of the ridge line of the subtropical anticyclone mark the outbreak of the ISM (Soman et al., 1993; Zhu et al., 2006).

Both the distributions of the geopotential heights at 700 hPa and the ridge line of the subtropical anticyclone at 500 hPa in Figure 1 show that the Arabian Peninsula is dominated by a middle-layer subtropical anticyclone during the ISM onset. On June 1–2 the subtropical anticyclone is weak and its ridge line is located near 20°N. From June 3 the ridge line of the subtropical anticyclone over the Arabian Peninsula begins to move northwards and reaches at 25°N
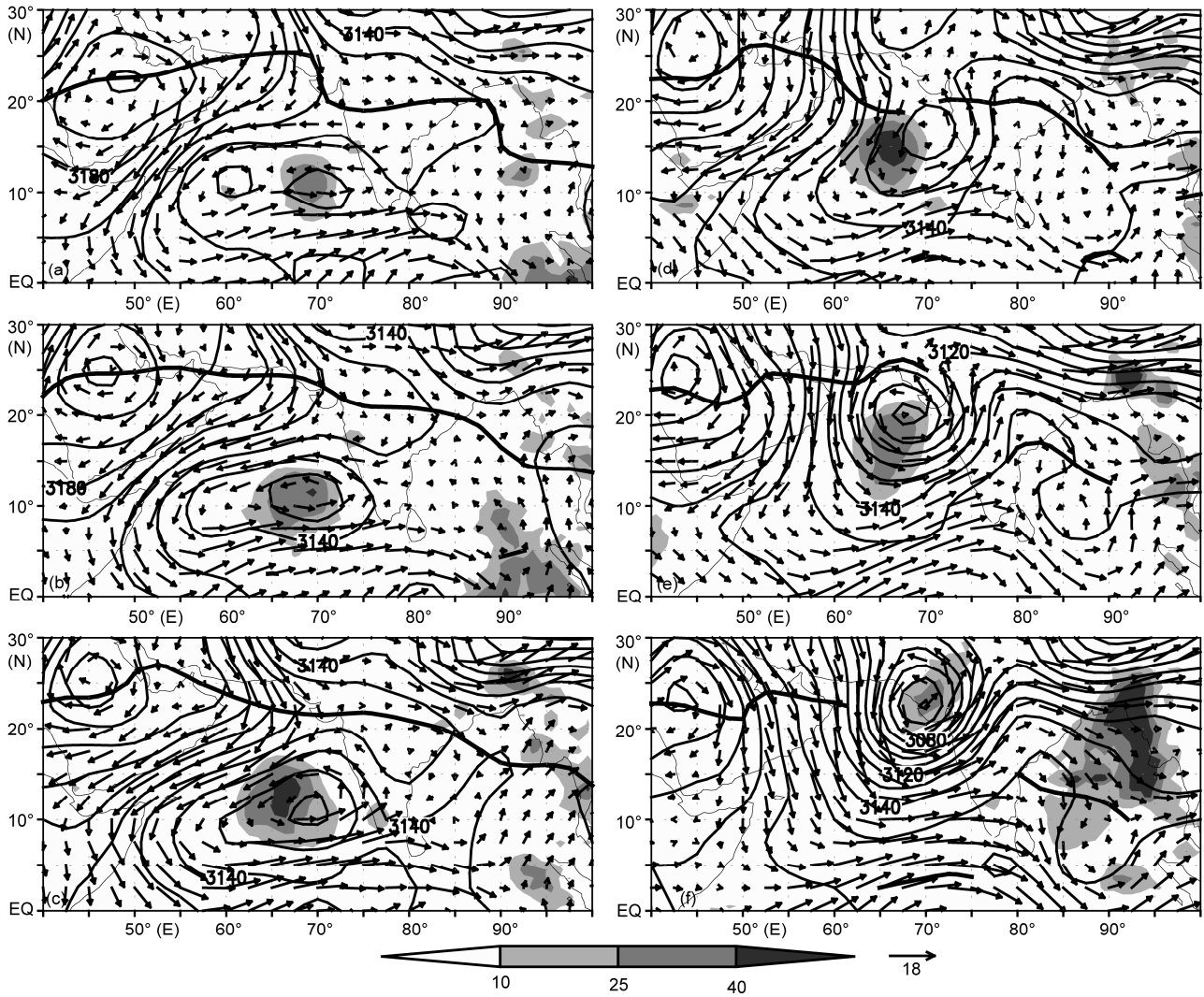
Figure 1   Distributions of daily precipitation, 700 hPa geopotential height and wind, and the ridge line of the 500 hPa subtropical anticyclone on June 4–9, 1998. Shade represent precipitation (unit: mm d^{-1}); thin solid and vector represent respectively 700 hPa geopotential height (unit: gpm) and wind (unit: m s^{-1}); thick solid represent the ridge line of the 500 hPa subtropical anticyclone.
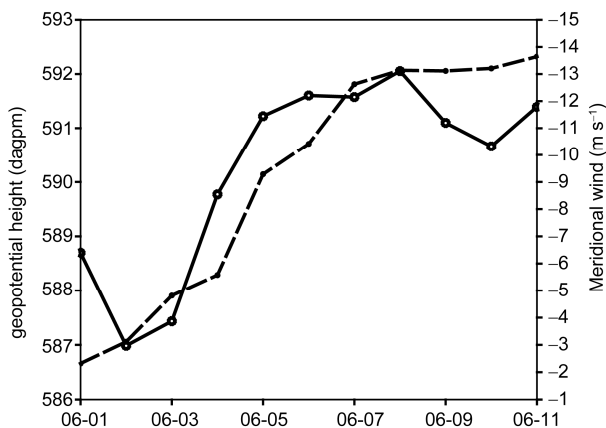
Figure 2   Evolutions of the 500 hPa geopotential height averaged over the Arabian Peninsula (35°–55°E, 15°–35°N) (solid, unit: dagpm) and meridional wind averaged over the Arabian Sea (55°–65°E, 15°–35°N) (dashed, unit: m s^{-1}).

by June 5 with its intensity increasing remarkably (Figure 1(b)). The subtropical anticyclone reaches its maximal strength and the northernmost location just before the onset on June 5–6, and begins to move southwards and weakens after the ISM onset on June 8. Figure 2 shows the evolution of mean geopotential height averaged over the Arabian Peninsula (35°–55°E, 15°–35°N) and the meridional wind averaged over a region on its east (55°–65°E, 15°–35°N) at 500 hPa, respectively. It shows that the subtropical anticyclone intensifies dramatically from June 3. Two days later (June 5) it strengthens slowly and maintains steady till the onset date with a geopotential height of 591–592 dgpm. At the same time, the northerlies over the Arabian Sea increase obviously from 2 to 12 m s^{-1} before the onset and maintain approximately 13 m s^{-1} after the onset. These all indicate that the subtropical anticyclone intensifies significantly before the ISM onset in 1998.

2.2 Westward extension and intensification of the SAH

Figure 3 shows evolution of daily rainfall, and the geopotential height, wind and the ridge line of the SAH at 200 hPa during the ISM onset. Before June 4, the SAH is weak with the west of its 12540 gpm located at 90°E (figure omitted). On June 4–5, the SAH begins to extend westwards, and at the onset date the 12540 gpm moves to the western part of the Indian Peninsula (Figure 3(a)–(d)). After the onset, the SAH extends westwards further and intensifies continuously (Figure 3(e), (f)). During the SAH westward extension, a cyclonic curvature occurs on the southwest of the SAH on June 6 near the rainy area and this curvature intensifies further on June 7. On June 8, the SAH center breaks and the rainy area appears under the southwest of the main part. After that with the SAH intensifying and moving westwards easterly flow on its south side strengthens and extends westwards to Arabia and Africa. The intensification

and westward moving of the SAH and the appearance of its two separate centers indicate that the ISM has been established (Zhu et al., 2006; Zhang et al., 2002).

The occurrence of cyclonic curvature of the SAH is found on its southwest side over the Arabian Sea on June 6–7 and the associated divergence is enhanced due to intensifying southerlies on the northeast side of the curvature and northerlies on its southeast side (Figure 3(c), (d)). The evolution of the divergence at 200 hPa (Figure 4) shows that the weak divergent area over the Arabian Sea is located at south of 15°N with the center at south of 10°N before June 4 (figure not shown). On June 5, the divergence strengthens obviously although the main part is still located at south of 15°N (Figure 4(b)). On June 6, the divergent area together with convections shift northwards remarkably (Figure 4(c)), and on June 7 these centers all move to north of 10°N. Due to the development of convection in middle and lower troposphere induced by upper-layer pumping associated with
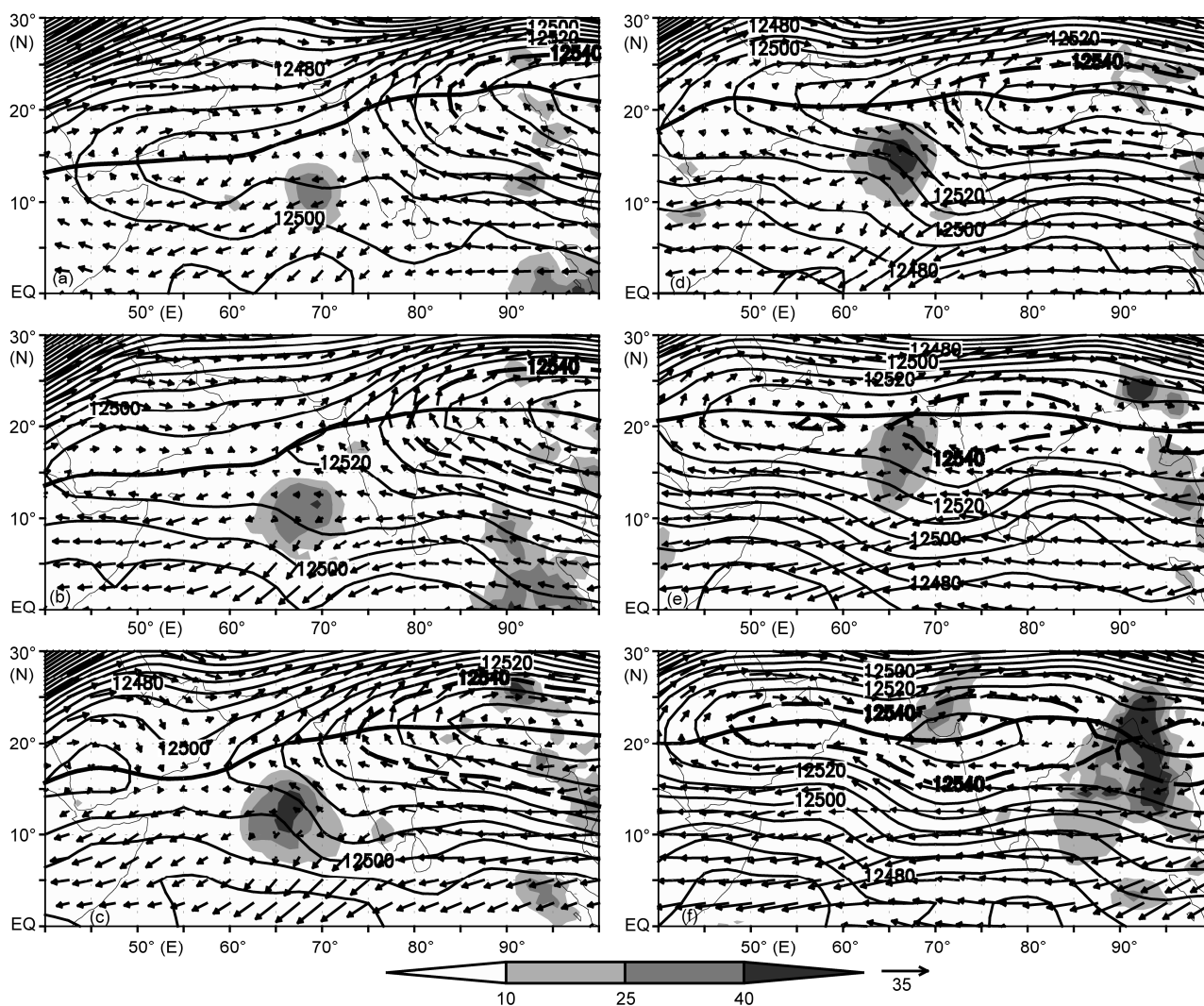
Figure 3 Distributions of daily precipitation (shaded, unit: mm d⁻¹), geopotential height (unit: gpm) and wind at 200 hPa (unit: m s⁻¹) on June 4–9, 1998. Thick solid line denotes the ridge line of the SAH and thick dashed one 12540 gpm.
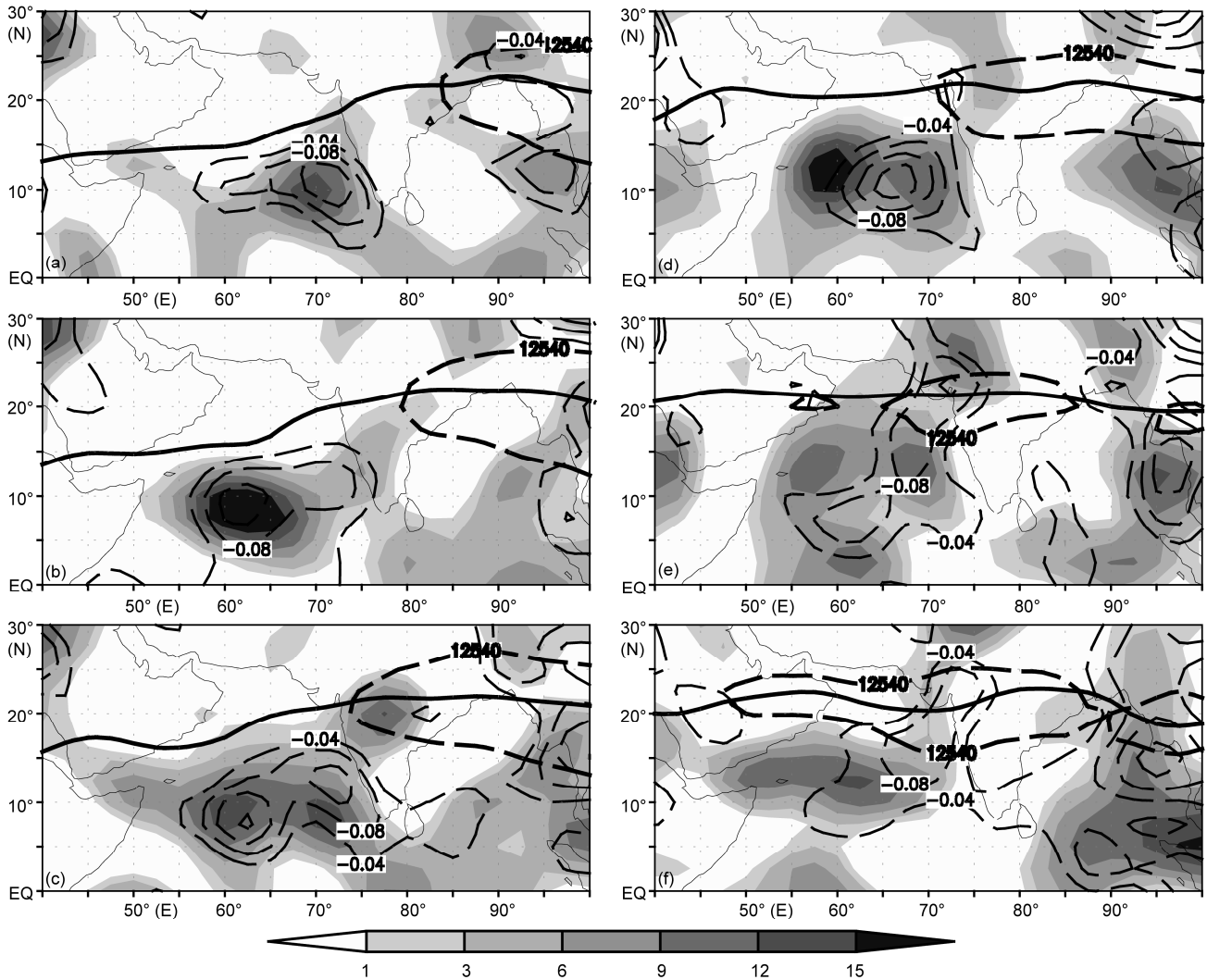
Figure 4 Distributions of divergence (shaded, unit: 10^{-6} s^{-1}) , contour 12540 gpm (thick dashed), and the ridge line of the SAH (thick solid) at 200 hPa and the pressure vertical velocity ω (dashed, unit: Pa s^{-1}) at 500 hPa on June 4–9, 1998.

the northward moving of the divergence, the tropical cyclone that is initially located near the equator moves northwards and intensifies as well.

The above analyses show that the tropical cyclone lingering near 10°N before the ISM onset is prevented from moving northwards by the subtropical anticyclone dominating the Arabian Sea and the Indian Peninsular. A cyclonic curvature on the southwestern SAH over the Arabian Sea occurs by June 6 and intensifies on June 7, resulting in maladjustment between pressure and wind fields. Outflow is induced by the Coriolis force due to the anomalous cyclonic flow, and the local divergence is formed in the upper troposphere, in favor of the northward moving of the tropical cyclone. Since the cyclone radius is less than 300 km and far less than the Rossby radius of deformation, pressure is adapted to the wind field, resulting in decreasing height and the shorter air column beneath it. Under the condition of adiabatic state, in order to maintain geostrophic and hydro-

static equilibria, air column becomes colder by virtue of atmospheric adiabatic ascent. Consequently the pumping in the upper troposphere is formed, leading to the intensification and northward moving of the tropical cyclone and the break of the ridge line of the subtropical anticyclone, which implies the ISM onset. In summary, it is the cyclonic curvature of the SAH on its southwestern side over the Arabian Sea that plays a very important role in triggering the ISM onset in 1998. In section 5, the mechanism concerning the variation of the SAH is explored based on potential vorticity (PV) analysis.

3 SAH variation triggered by diabatic heating before the ISM onset in 1998

3.1 The triggering effects of latent heating on SAH

In 1998, the BOB monsoon onset was on May 15 (Mao,

2001; Liu et al., 2003a, Yan, 2005; Wu et al., 2011) and the SCS monsoon onset was on May 21 (Ding et al., 1999; He et al., 1999; Chen et al., 1999). Afterwards, the rainfall over southeastern Asia increased dramatically, forming a strong latent heat to the atmosphere. In subtropical area, the Sverdrup relationship (Wu et al., 2000; Wu et al., 2003; Liu et al., 2004) between diabatic heating and meridional wind is as follows:

$$\beta v \approx \theta_z^{-1}(f + \zeta)\, Q_z,\ \theta_z \neq 0. \tag{7}$$

Above the maximum heating of a deep convective condensation, heating decreases with height and negative vorticity is generated. In subtropical area where vorticity advection is weak, in order to maintain local vorticity balance positive planetary vorticity advection is required. Consequently northerly is generated above the heating region and anticyclonic vorticity is produced on its western side. In other words, the unstable development of the SAH is induced by the strong monsoon latent heating over East Asia. This development of zonal asymmetric instability (Hsu et al., 2000; Popovic et al., 2001) is accompanied with high PV eddies moving southwards continuously on the eastern side of the high then being transported westward along the easterlies on its south side, forming a high PV belt there. High PV eddies are shed continuously from this high PV belt. Can these high PV eddies contribute to the variation of the SAH and further trigger the onset of the ISM? Before discussing these problems, the variations of latent heating and the SAH before the ISM onset are explored.

Figure 5 is the horizontal distribution of rainfall and geopotential height at 200 hPa from the 27th to 31th pentads in 1998. Before the BOB monsoon onset in the 27th pentad (Figure 5(a)), there is little precipitation in the region from BOB to SCS and the center of the SAH is located over the south of Indo-China Peninsula. After the BOB monsoon onset in the 28th pentad (Figure 5(b)), the rainfall over BOB increases and the latent heating strengthens (Zhang et al., 2009). At the same time, the SAH also intensifies. By the 29th pentad (Figure 5(c)) the onset of SCS monsoon occurs with increasing rainfall over the SCS. At the same time the SAH reinforces and moves westwards obviously with its 12560 gpm westward extending to the Arabian Sea. Afterwards by the 30th pentad (Figure 5(d)), with the development of the East Asia monsoon, the rainy area and the SAH both extend northeastwards. Owing also to the precipitation over the Northwest Pacific in the early days, the SAH has extended northeastwards to east of 140°E, and further to east of 160°E before the onset of the ISM (the 31th pentad, Figure 5(e)). During the northeastward development of the SAH, high PV moves southwestward advected by northerlies from the mid-ocean trough on the eastern side of the SAH (Guo et al., 2008).

After the onset of the BOB and the SCS monsoon, latent heating becomes important with its center being located in middle layers. This vertical distribution of heating can intensify northerlies in the upper troposphere (Zhang et al., 2009; Liu et al., 1999b). It is possible that the zonal asymmetric instability is induced and the variation of the SAH is stimulated. Bearing these in mind, in next section we will discuss the effects on the variation of the SAH and the ISM onset of the westward propagating high PV eddies along the high PV belt on the south of the SAH.

3.2 The effects on the subtropical anticyclone of the surface sensible heating over the Arabian Peninsular

Figure 6 demonstrates the variations of surface sensible heat flux and near surface potential temperature averaged within 10°–20°N in 1998. It shows that sensible heating over the Indian and Arabian Peninsula is strong with an intensity of more than 120 W m^{-2} (Figure 6(a)) from March to May. Over the Indian Peninsula, the surface sensible heat flux decreases in May and becomes less than 90 W m^{-2} by mid-May. On the contrary, over the Arabian Peninsula it maintains more than 90 W m^{-2}. After early June, sensible heating decreases clearly over both Peninsulas, especially over the Indian Peninsula where it weakens apparently owing to the development of the monsoon vortex and the ISM onset. In short, sensible heating over the Arabian Peninsula remains strong before the ISM onset and is even stronger than over the Indian Peninsula in mid and late May. The same conclusion is obtained by using the ECMWF ERA-40 reanalysis data (figure not shown) and demonstrates that the characteristics of the strong sensible heating over the Arabian Peninsula before the ISM onset are at least qualitatively reliable.

Because the Arabian Peninsula altitude is higher than the Indian Peninsula, thermal effect of the same heating on atmosphere is obviously different. Figure 6(b) shows that Arabian Peninsula is warmer than the Indian Peninsula with maximum potential temperature of up to 315 K, especially before the ISM onset, which implies that sensible heating over the Arabian Peninsula cannot be ignored. According to the thermal adaption theory (Wu et al., 1999; Liu et al., 1999a), sensible heating can generate low-level cyclone and upper-level anticyclone. We can thus infer that the strong sensible heating on the Arabian Peninsula is very important to the enhancement of the local subtropical anticyclone.

4 The impacts on the ISM onset of subtropical anticyclone instability induced by diabatic heating

4.1 The impacts of the SAH instability induced by latent heating

The vertical cross sections of PV (figure omitted) indicate that the 355 K isentropic surface is close to 200 hPa in the
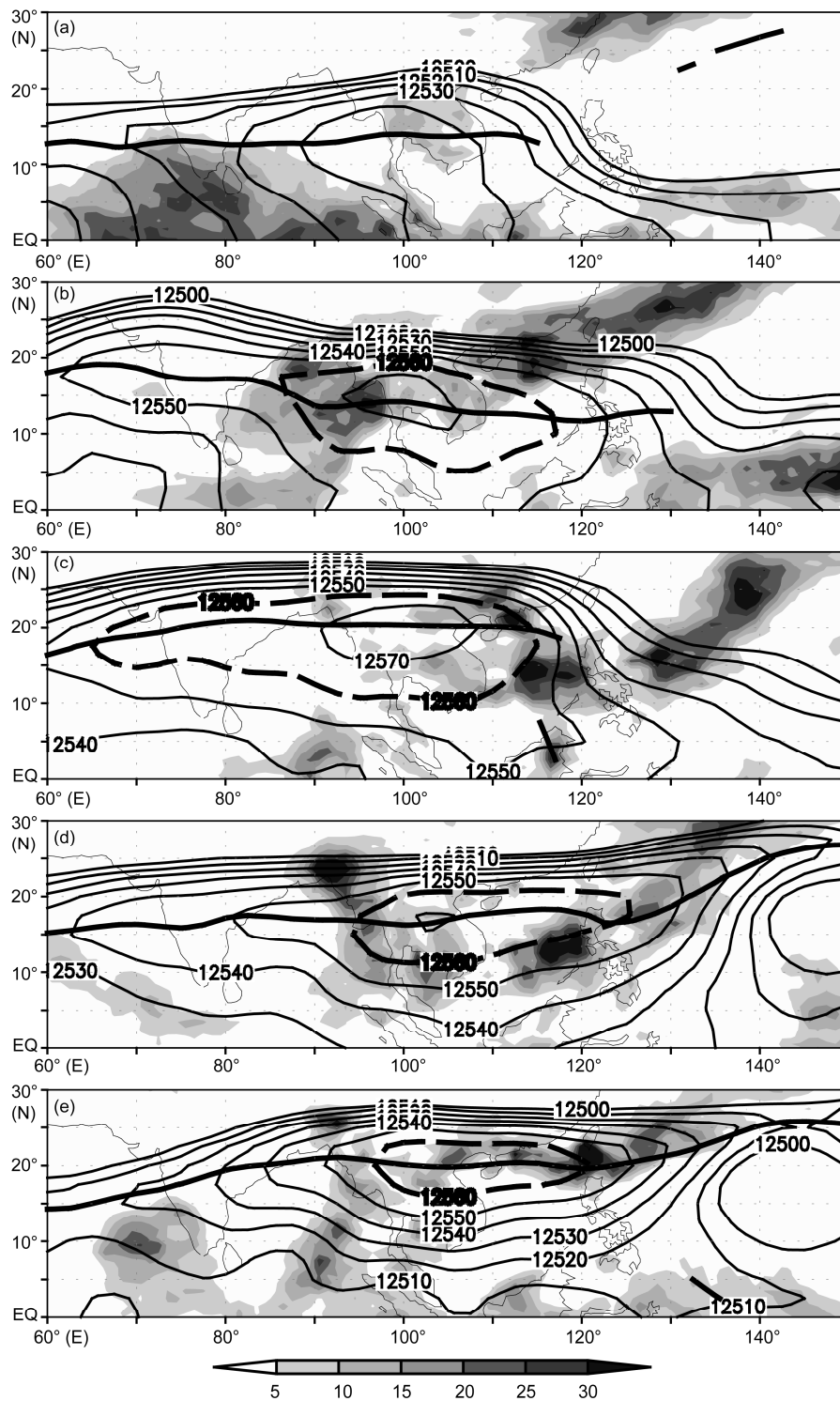
Figure 5 Distributions of pentad mean precipitation (shaded, unit: mm d^{-1}) and 200 hPa geopotential height (unit: gpm) during the 27th to 31th pentads in 1998. Thick solid denotes the ridge line of the SAH and thick dashed denotes the 12560 gpm contour. (a) 27th pentad (May 11 to 25), (b) 28th pentad (May 16 to 20), (c) 29 th pentad (May 21 to 25), (d) 30th pentad (May 26 to 30), (e) 31st pentad (May 31 to June 4).

subtropics and the variation of PV at this surface has the most significant impacts on the SAH. So in the following we focus on the variation of PV at the 355 K surface.

The above analyses show that from May 31 to June 4 the SAH develops quietly and extends to the east of 160°E and

that the unstable development of the SAH can lead to high PV eddies moving southwards along the strong northerlies to its east then westwards from the Mid-ocean trough. Figure 7 demonstrates the distributions of PV and wind field at 355 K on May 27 and June 4, 1998. The aforementioned
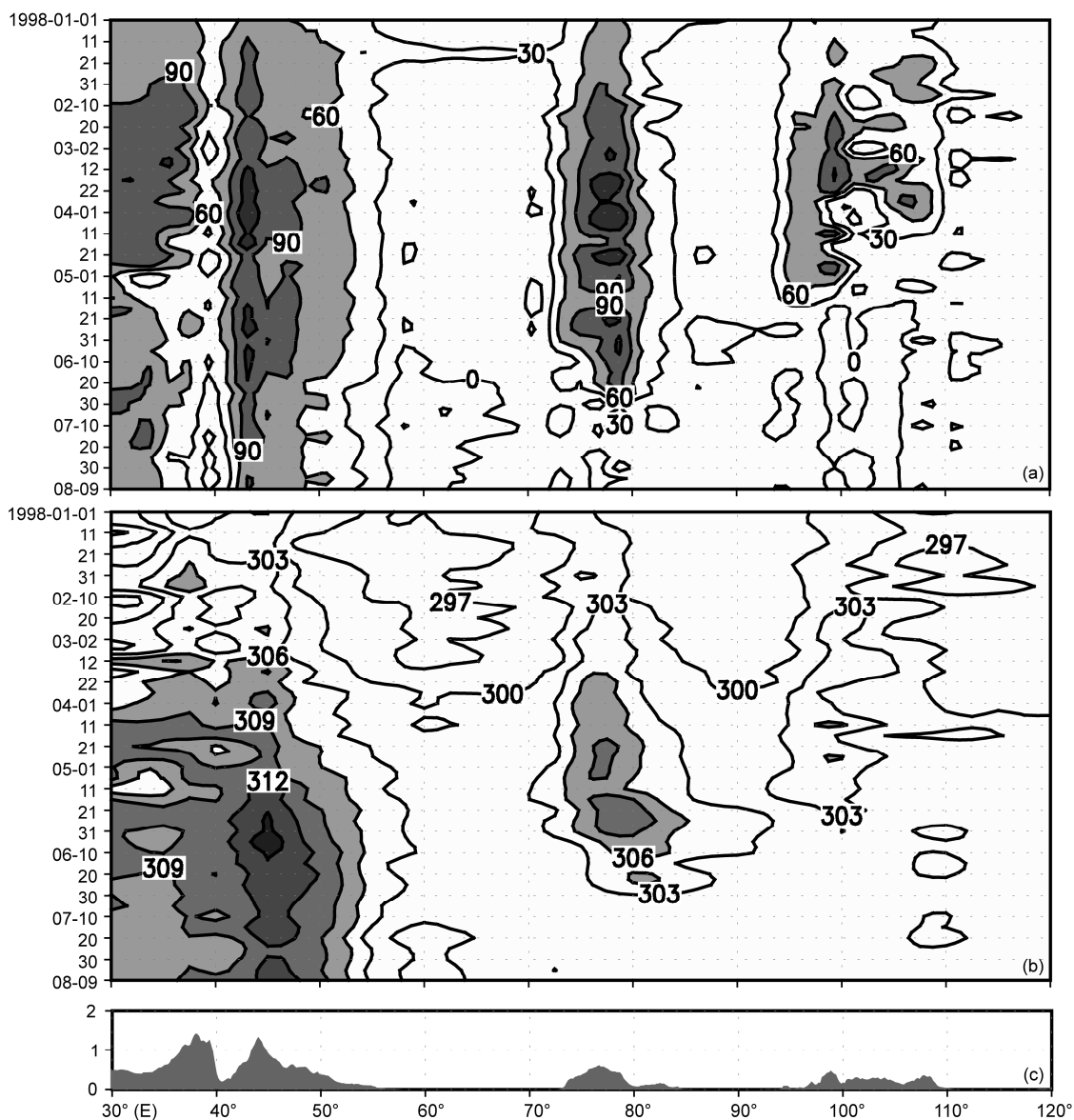
Figure 6 Evolutions from January to August in 1998 (ordinate) of (a) surface sensible heat flux (unit: W m^{-2}) and (b) near surface (σ=0.995) potential temperature (unit: K) averaged over 10°–20°N. (c) is the corresponding terrain height (unit: km).

processes are clearly presented: the high PV is located near 130°E on 27 May and is advected to 110°E on June 4 due to the eastward extension and intensification of the SAH.

Figure 8 shows the distributions from June 5 to 8 of PV and wind field at 360 K, 355 K and 330 K, which can well present the characteristics of the upper and middle troposphere. On June 5 (Figure 8(a) and (e)), the SAH extends eastwards with a low PV area lying near 120°–140°E. Over the southeast of the low PV, the high PV at high latitude moves southwestward along the northeasterly which prevails from northwest Pacific via Japan to the SCS. On the southwest side of the SAH, the high PV is transported northwestwards along the southeasterly. Thus, a high PV belt is formed around the southern anticyclone, and is eventually connected with the high PV embedded in the

westerly trough at middle-high latitudes on the northwest side of the anticyclone. This phenomenon is most obvious at 370 K (figure not shown) with a mostly continuous high PV belt, but becomes weaker with decreasing height. At 355 K, it is displayed by a series of isolated high PV eddies (Figure 8(e)–(h)). At 330 K (Figure 8(i)–(l)), the high PV eddies almost disappear on its south side. However, on the western side of the SAH, they are still obvious and connected with the westerly trough to the north, constituting a pattern of 'North Trough and South Vortex'. These enable the high PV in higher latitudes to be transported to low latitudes effectively.

On June 6 at 355 K (Figure 8(f)), there are two high PV eddies, denoted respectively as P1 and P2, which are transported westwards to the Arabian Sea and the Indian Penin-
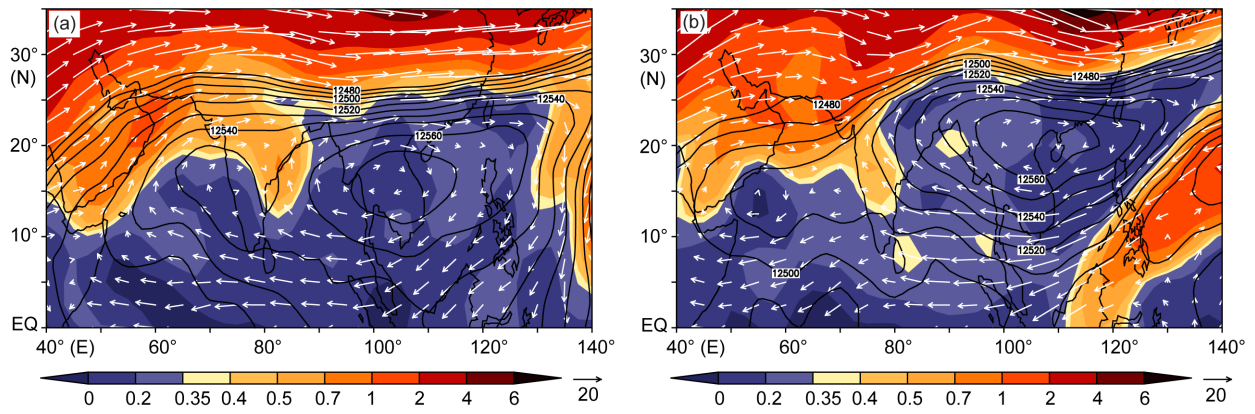
Figure 7 Distributions of PV (shaded, unit: PVU) and wind field (unit: m s^{-1}) at 355 K and geopotential height at 200 hPa (unit: gpm). (a) May 27; (b) June 4.
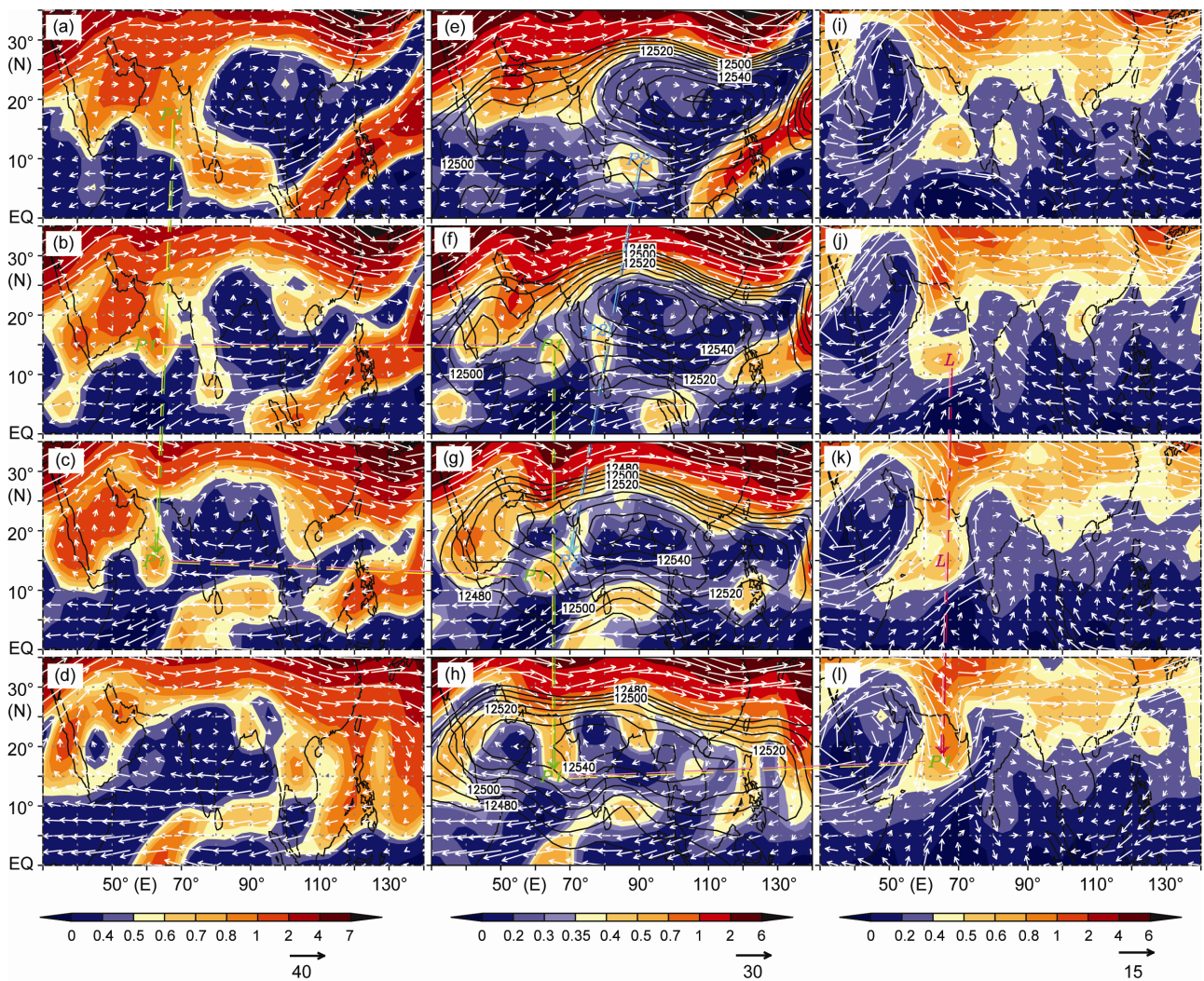
Figure 8 Evolutions from June 5 to 8, 1998 (from the first row down to the fourth row) of the PV (shading, unit: PVU), wind (vector, unit: m s^{-1}), and the geopotential height at 200 hPa (solid curve, unit: gpm) at 360 K ((a)–(d)), 355 K ((e)–(h)), and 330 K ((i)–(l)). Vertical dashed arrows indicate the horizontal movements of the vortex P1 and P2 in the upper troposphere and the low pressure system L in the middle troposphere; while the horizontal pink and long-dashed arrows indicate the vertical phase-lock and baroclinic development of the vortex system.

sula along the high PV belt on the south side of the SAH. The P1 is located just over the southwest side of the SAH

where the cyclonic curvature occurs. This is because the advection of positive PV can force cyclonic circulation

anomaly (Hoskins et al., 1985). The southerlies on the northeast and the northerlies on the southwest side of the P1 both increase, leading to the intensification of the local divergence. Such an intense upper layer pumping owing to the divergence can stimulate the development of convection in the lower layers and help the northward movement and development of the cyclone existed in the tropics.

On June 7 (Figure 8(g)), the P2 moves northwestward to 15°–20°N and weakens slightly, while the P1 moves slowly and intensifies greatly. Consequently the P1 and P2 merge together to form a northeast-southwest oriented high PV belt. At the same time, the cyclonic curvature on the southwest of the SAH extends northeastwards, in favor of the northward development of the low-layer tropical cyclone (Figure 1(d)). The vertical cross sections of PV from June 6 to June 7 (Figure 9) reveal that the intensification of the P1 at 355 K on June 7 is mainly related to the southward and downward extending of the upper-layer high PV. On June 6, there is a high PV area over 60°–65°E in the upper troposphere that tilts westwards with increasing height, with a PV of 0.5 PVU at 355 K (Figure 9(a) and (b)). On June 7, this high PV develops clearly downward, and its center near 12.5°N at 355 K increases to 0.6 PVU (Figure 9(c) and (d)). Notice that the temperature near 65°E at 200 hPa increases slightly, implying that the latent heating resealed from the developing cyclone in the lower layers also contributes to the P1 intensification. Under the forcing of the upper-layer high PV, the tropical cyclone in the middle and lower troposphere begins to move northwards and intensifies, presenting a vertical phase-lock between the upper and lower circulations and baroclinic development of the vortex system. On June 6, the high PV center in the middle and lower troposphere is located near (67°E, 12°N) (Figure 8(j) and Figure 9(a)), and the P1 center at 360 K in the upper troposphere is located near (62°E, 17°N) (Figure 8(b)). By June 7, the former moves northwards to (67°E, 15°N) (Figure 9(d)) and the latter develops downwards and southwards. At the same time, The P2 at 355 K which is originally located at the southern tip of the Indian Peninsula (June 6) is advected northwestward to (15°N, 65°–70°E) and merges with the P1 (Figure 8(g)). On June 8, in the upper troposphere, the high PV near the P1 at 355 K moves to the northern Arabian Sea (Figure 8(h)), and the high PV areas expand further. In the middle troposphere, the low-latitude high PV at 330 K moves to the same area (Figure 8(l)), almost overlapping with the upper-layer high PV and forming a barotropic structure under 360 K (Figure 9(e)). The deep convection develops most greatly and huge latent heat is released. The temperature at 200 hPa increases significantly and reaches to 360 K (Figure 9(e)). It becomes apparent that the development of high PV over the northern Arabian Sea at 355 K as shown in Figure 8(h) is mainly a result of condensation heating.

In conclusion, the high PV eddy shedding from the high PV belt induced by the unstable development of the SAH in the upper troposphere moves northwestwards along the basic flow after it reaches the southwest side of the anticyclone. By June 6–7, it arrives in the Arabian Sea and leads to a cyclonic curvature of the SAH, which results in an intensified upper-layer divergence, the northward movement of the tropical cyclone in the lower layers, and eventually the onset of the ISM. The above analyses show that the northward movement and the rapid development of the tropical cyclone in the middle and lower troposphere are the consequence of the westward migration and intensification of the SAH, the development of the PV zonal asymmetric instability, and the formation of the upper-layer pumping on the southwest side of the SAH which all together lead to the high PV phase-lock between the upper and lower circulations and the baroclinic development of the vortex system. That high PV moves from northeast to southwest, and further turns to northwest on the south side of the SAH is more clearly observed in the upper troposphere, where the transported high PV can also induce the development of positive PV anomalies in the lower layers (Hoskins et al., 1985).

4.2 Development of subtropical anticyclone due to surface sensible heating of the Arabian Peninsula and its impacts on the ISM onset

The analyses in section 3 show that prior to the onset of the ISM, there is strong surface sensible heating on the Arabian Peninsula and rapid intensification of subtropical anticyclone in the middle-layer. Does this affect the ISM onset and what is its role? Distributions of PV at 330 K (Figure 8(i)–(l)) indicate that there has been a low PV area over the Arabian Peninsula in accordance with the persistent subtropical anticyclone at 500 hPa (figure not shown). There are two high PV regions on the eastern side of the subtropical anticyclone. One lies to the north of 20°N which is advected southward later. The other is a low-latitude tropical system and located near 10°–15°N. They together form the structure of 'North Trough and South Vortex' (Figure 8(i) and (j)). As the subtropical anticyclone strengthens with time, the northerlies to its east intensify (Figure 2). The advected high PV from high latitude extends southwards continuously and finally a high PV belt forms on the east side of the subtropical anticyclone which can reach Northern Africa along the anticyclonic circulation. When the high PV extends southward and the trough over the Arabian Sea deepens, the previous subtropical anticyclone that dominated over the Arabian Sea retreats westwards towards the Arabian Peninsula (Figure 1(b)–(f)). Afterwards, the tropical cyclone in front of the trough begins to move northwards (Figure 8(k) and (l)), and the barotropic development of 'North Trough and South Vortex' occurs along the west coast of India (Hoskins et al., 1985), and the development of the low-level cyclone in the Arabian Sea thus triggers the onset of the ISM (Mao, 2001; Krishnamurti et al., 1981; Soman, 1993). Therefore, except for the pumping of the
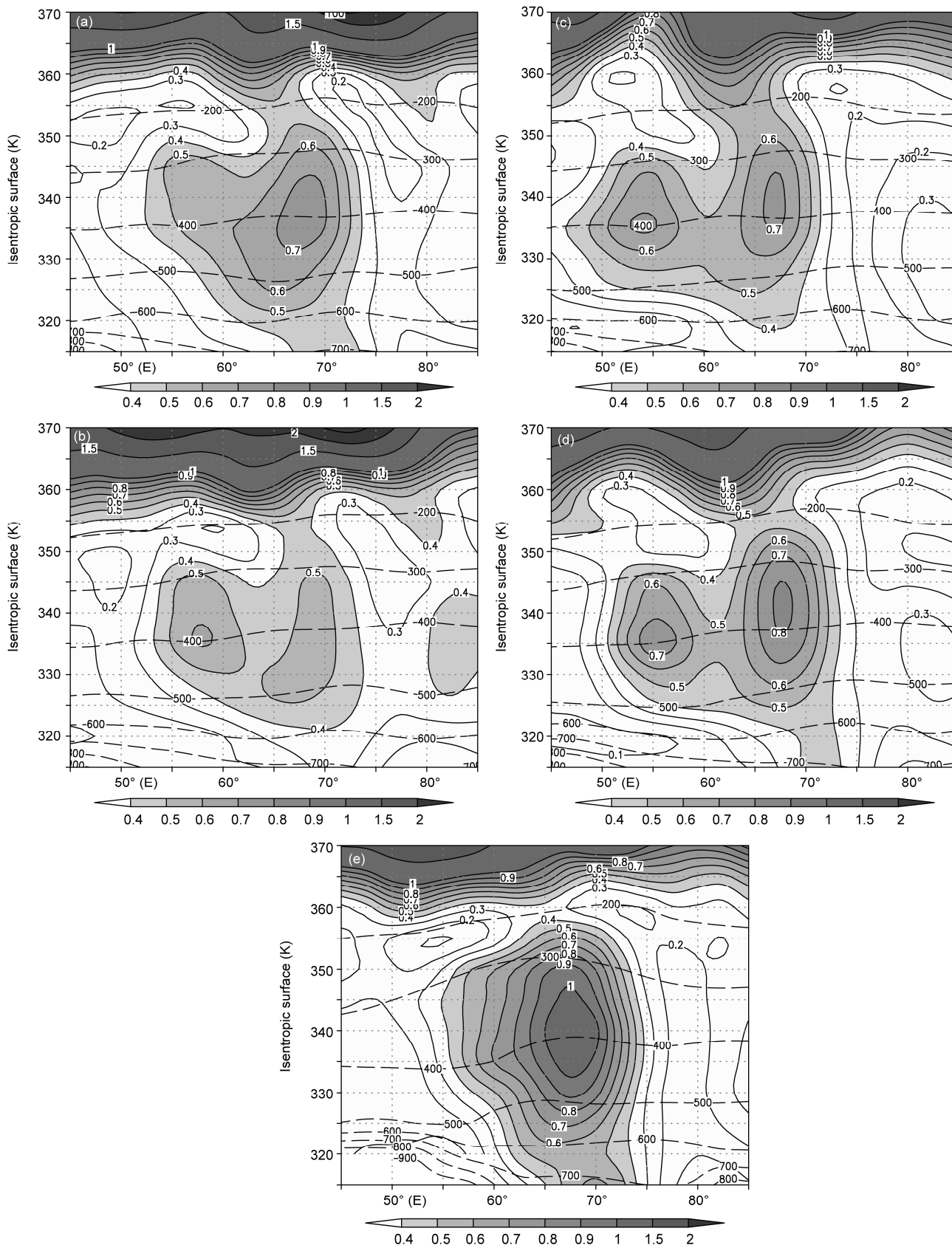
Figure 9 Vertical cross sections of the PV (solid and shaded, unit: PVU) and isobaric surface (dashed, unit: hPa) at 12.5°N ((a), (c)), 15°N ((b), (d)) , and 20°N (e) on June 6 ((a), (b)), 7 ((c), (d)) and 8 (e), 1998.

upper-layer divergent circulation, the deepening of the middle-layer high PV trough also has impacts on the ISM onset, which is related to the westward retreat and intensification of the anticyclone over the Arabian Sea and the Arabian Peninsula area.

5 Discussion and conclusions

Based on a case in 1998, the development of the SAH instability induced by diabatic heating and its impacts on the ISM onset are studied, and the main reason of the ISM onset is investigated. The main conclusions are as follows:

The latent heating released from the strong rainfall over BOB and SCS as well as the western Pacific make the SAH enhance dramatically prior to the ISM onset. On the eastern side of the SAH the high PV at high latitudes moves southwards along the northerlies. As a result, a high PV belt forms on the east of the SAH and the zonal asymmetric forcing of PV appears. The high PV belt extends westward to the northwest side of the SAH along the easterlies on its south. High PV eddies are shed from the belt and transported westwards continuously along this belt, forming the main source of positive PV anomalies in the upper troposphere. At 355 K high PV eddies are also advected westward to the Arabian Sea from the northeastern side of the SAH, contributing to the development of cyclonic curvature and the enhancement of divergence on the southwest of the SAH, forming an upper-level pumping. The northward moving tropical cyclone in the lower layers thus develops abruptly, leading to the onset of the ISM. In short, the phase-lock between the upper and lower circulations and the baroclinic development of the vortex system are the main mechanism of the rapid intensification of the northward moving tropical cyclone.

The intensification of the middle-layer anticyclone over the Arabian Peninsula is another factor leading to the onset of the ISM. Before the onset, the strong surface sensible heating is maintained on the Arabian Peninsula. This causes the middle-level subtropical anticyclone lying over the Arabian Sea in spring retreats westwards and enhances over the Arabian Peninsula, and the zonal asymmetric instability of PV develops gradually. The high PV in high latitudes moves southwards along the northerlies on the east of the subtropical anticyclone and a high PV trough comes into being in the middle troposphere over the Arabian Sea, in favor of the northward migration of the tropical cyclone and its barotropic development into a monsoon onset vortex.

From the case analyses of 1998, the ISM onset dynamics can be summarized as follows. First, due to the strong latent heating over East and Southeast Asia after the BOB and SCS monsoon onset, the SAH experiences unstable development and expands eastward and westward; the zonal asymmetric development of PV forcing is stimulated. Second, high PV from high latitudes is advected southwards

and high PV eddies are shed and transported westwards to the Arabian Sea around the SAH, forming divergence and pumping in the upper troposphere, which is favorable to the northward moving and baroclinic development of the tropical cyclone in the lower troposphere. At the same time, due to the strong sensible heating over the Arabian Peninsula, a local anticyclone develops in the middle layers. To its east, the positive advection of PV along the enhanced northerlies over the Arabian Sea provides a favorable background for the northward movement of the tropical cyclone and its barotropic development. Eventually, under the above circulations in the middle and upper troposphere, the cyclone originally lying at the southern Arabian Sea jumps northwards and develops explosively into an intense vortex which leads to the onset of the ISM.

Although the above conclusions are obtained based only on the 1998 case, they are still instructive in general. This is because there generally exist the latent heat release of the BOB and SCS monsoon, which drives the unstable development of the SAH, and the strong sensible heating, which generates the middle-layer subtropical anticyclone over the Arabian Peninsula. However, there are also many other factors affecting the onset of the ISM, such as the gradient of cross-equatorial sea surface temperature, the air-sea interaction in the Arabian Sea, the thermal contrast of Indian continent and nearby oceans, and the ENSO events, etc. How the mechanism revealed in this study and the other factors work together to affect the ISM onset and its inter-annual variation is still unclear and deserves further studies.

Chen L X, Zhu C W. 1999. Characteristics and mechanism analysis of the SCS summer monsoon onset during SCSMEX in 1998 (in Chinese). In: Li C Y, ed. Onset and Evolution of the South China Sea Monsoon and its Interaction with the Ocean. Beijing: China Meteorological Press. 13–17

Ding Y H, Xue J S, Wang S R, et al. 1999. The onset and activities of Asian monsoon and heavy flooding in China in 1998 (in Chinese). In: Li C Y, ed. Onset and Evolution of the South China Sea Monsoon and its Interaction with the Ocean. Beijing: China Meteorological Press. 1–4

Ding Y H, Liu Y Y. 2008. A study of the teleconnections in the Asia-Pacific monsoon region. Acta Meteor Sin, 22: 404–418

Emanuel K A. 1995. On thermally direct circulations in moist atmospheres. J Atmos Sci, 52: 1529–1534

Ertel H. 1942. Ein neuer hydrodynamischer wirbelsatz. Meteor Z, 6: 277–281

Guo L, Liu Y M. 2008. The effects of diabatic heating on asymmetric instability and the Asian extreme climate events. Meteor Atmos Phy, 100: 195–206

Guo Q Y. 1992. Teleconnection between the floods/droughts in north China and Indian summer monsoon rainfall (in Chinese). Acta Geograph Sin, 47: 394–402

He J H, Wang L J, Xu H M. 1999. Abrupt change in elements around 1998

SCS summer monsoon establishment with analysis of its onset (in Chinese). In: Li C Y, ed. Onset and Evolution of the South China Sea Monsoon and its Interaction with the Ocean. Beijing: China Meteorological Press. 30–33

Held I M, Hou A Y. 1980. Nonlinear axially symmetric circulations in a nearly inviscid atmosphere. J Atmos Sci, 37: 515–533

Holton J R. 2004. An Introduction to Dynamic Meteorology. 4th ed. California: Elsevier Academic Press. 535

Hoskins B J, Mclntyre M E, Robertson A W. 1985. On the use and significance of isentropic potential vorticity maps. Quart J Roy Meteor Soc, 111: 877–946

Hsu C J, Plumb R A. 2000. Nonaxisymmetric thermally driven circulations and upper-tropospheric monsoon dynamics. J Atmos Sci, 57: 1255–1276

Jiang X, Li J. 2011. Influence of the annual cycle of sea surface temperature on the monsoon onset. J Geophys Res, 116: D10105, doi: 10.1029/2010JD015236

Kistler R, Kalnay E, Collins W, et al. 2001. The NCEP-NCAR 50-years reanalysis: Monthly means CD-ROM and documentation. Bull Amer Meteor, 82: 247–267

Krishnamurti T N, Ardanuy P, Ramanathan Y, et al. 1981. The onset-vortex of the summer monsoon. Mon Weather Rev, 109: 344–363

Li J P, Wu G X, Hu D X. 2011. Ocean-Atmosphere Interaction over the Joining Area of Asia and Indian-Pacific Ocean (in Chinese). Beijing: Meteorological Press. 1081

Liang P D. 1988. The Indian summer monsoon and the rainfall in north China in summer (in Chinese). Acta Meteor Sin, 46: 75–81

Lindzen S R, Hou A Y. 1988. Hadley circulation for zonally averaged heating centered off the equator. J Atmos Sci, 45: 2416–2427

Liu Y M, Chan J C L, Mao J Y, et al. 2003a. Impacts of the onset of the Bay of Bengal monsoon on the onset of the South China Sea monsoon, Part I: A case study (in Chinese). Acta Meteor Sin, 61: 1–9

Liu Y M, Chan J C L, Wu G X. 2003b. Impacts of the onset of the bay of Bengal monsoon on the onset of the South China Sea monsoon, Part II: Numerical experiments (in Chinese). Acta Meteor Sin, 61: 10–19

Liu Y M, Hoskins B J, Blackburn M. 2007. Impact of Tibetan orography and heating on the summer flow over Asia. J Meteor Soc Japan, 85B: 1–19

Liu Y M, Liu H, Liu P, et al. 1999a. The effect of spatially nonuniform heating on the formation and variation of subtropical high, Part II: Land surface sensible heating and East Pacific subtropical high (in Chinese). Acta Meteor Sin, 57: 385–396

Liu Y M, Wu G X, Liu H, et al. 1999b. The effect of spatially nonuniform heating on the formation and variation of subtropical high, Part III: Condensation heating and South Asia high and Western Pacific subtropical high (in Chinese). Acta Meteor Sin, 57: 525–538

Liu Y M, Wu G X, Liu H, et al. 2001. Condensation heating of the Asian Summer Monsoon and the subtropical anticyclones in the eastern hemisphere. Clim Dyn, 17: 327–338

Liu Y M, Wu G X, Ren R C. 2004. Relationship between the subtropical anticyclone and diabatic heating. J Clim, 17: 682–698

Liu Y Y, Ding Y H. 2008a. Teleconnection between the Indian summer monsoon onset and the Meiyu over the Yangtze River Valley. Sci China Ser D-Earth Sci, 51: 1021–1035

Liu Y Y, Ding Y H. 2008b. Analysis and numerical simulations of the teleconnection between Indian summer monsoon and precipitation in North China. Acta Meteor Sin, 22: 489–501

Mao J Y. 2001. Variation in the configuration of subtropical anticyclone during seasonal transition and the mechanism of Asian monsoon onset (in Chinese). Doctoral Dissertation. Beijing: Graduate University of Chinese Academy of Sciences

Plumb R A, Hou A Y. 1992. The response of a zonally symmetric atmosphere to subtropical thermal forcing: Threshold behavior. J Atmos Sci, 49: 1790–1799

Popovic J M, Plumb R A. 2001. Eddy shedding from the upper-tropospheric Asian monsoon anticyclone. J Atmos Sci, 58: 93–104

Schneider E K. 1977. Axially symmetric steady-state models of the basic state for instability and climate studies, Part II: Nonlinear calculations. J Atmos Sci, 34: 280–297

Schneider E K. 1987. A simplified model of the modified Hadley circulation. J Atmos Sci, 44: 3311–3328

Sobel A H, Plumb R A. 1999. Quantitaive diagnostics of mixing in a shallow water model of the stratosphere. J Atmos Sci, 56: 2811–2829

Soman M K, Kumar K K. 1993. Space-time evolution of meteorological features associated with the onset of Indian summer monsoon. Mon Weather Rev, 121: 1177–1194

Wu G X, Guan Y, Liu Y M, et al. 2012. Air-sea interaction and formation of the Asian summer monsoon onset vortex over the Bay of Bengal. Clim Dyn, 38: 261–279

Wu G X, Guan Y, Wang T M, et al. 2011. Vortex genesis over the Bay of Bengal in spring and its role in the onset of the Asian Summer Monsoon. Sci China: Earth Sci, 54: 1–9

Wu G X, Liu H. 1998a. Vertical vorticity development owing to down-sliding at slantwise isentropic surface. Dyn Atmos Ocean, 27: 715–743

Wu G X, Liu Y M. 2000. Thermal adaptation, overshooting, dispersion and subtropical anticyclone, Part I: Thermal adaptation and overshooting (in Chinese). China J Atmos Sci, 24: 433–446

Wu G X, Liu Y M. 2003. Summertime quadruplet heating pattern in the subtropics and the associated atmospheric circulation. Geophys Res Lett, 30: 1201–1204

Wu G X, Liu Y M, Liu P. 1999. The effect of spatially nonuniform heating on the formation and variation of subtropical high, Part I: Scale analysis (in Chinese). Acta Meteor Sin, 57: 257–263

Wu G X, Zhang Y S. 1998b. Tibetan Plateau forcing and the timing of the monsoon onset over South Asia and the South China Sea. Mon Weather Rev, 126: 913–927

Xie S P, Saiki N. 1999. Abrupt onset and slow seasonal evolution of summer monsoon in an idealized GCM simulation. J Meteor Soc Japan, 77: 949–968

Yan J H. 2005. Asian summer monsoon onset and advancing process and the variation of the subtropical high (in Chinese). Doctoral Dissertation. Beijing: Graduate University of Chinese Academy of Sciences

Zhang Q, Wu G X, Qian Y F. 2002. The bimodality of the 100hPa South Asia High and its relationship to the climate anomaly over East Asia in summer. J Meteor Soc Japan, 80: 733–744

Zhang Y N, Liu Y M, Wu G X. 2009. Stationary response of the subtropical circulation to latent heating in a linear Quasigeostrophic model, Part I: Basic quality and characteristic analysis (in Chinese). China J Atmos Sci, 33: 868–878

Zhang Y S, Wu G X. 1998. Diagnostic investigations of mechanism of onset of Asian summer monsoon and abrupt seasonal transitions over northern hemisphere, Part I: Stages of summer monsoon onset (in Chinese). Acta Meteor Sin, 56: 513–528

Zheng X Y. 1998. The response of a moist zonally symmetric atmosphere to subtropical surface temperature perturbation. Quart J Roy Meteor Soc, 124: 1209–1226

Zhu M, Zhang M. 2006. Evolution character of flow field during onset phase of the Indian summer monsoon (in Chinese). J PLA Univ Sci and Technol, 7: 189–194